

Comparison of Two Epochs of the Zeeman Effect in the 44 GHz Class I methanol (CH_3OH) maser line in OMC-2

E. Momjian¹, A. P. Sarma²

ABSTRACT

We present a second epoch of observations of the 44 GHz Class I methanol maser line toward the star forming region OMC-2. The observations were carried out with the Very Large Array, and constitute one of the first successful Zeeman effect detections with the new WIDAR correlator. Comparing to the result of our earlier epoch of data for this region, we find that the intensity of the maser increased by 50%, but the magnetic field value has stayed the same, within the errors. This suggests that the methanol maser may be tracing the large-scale magnetic field that is not affected by the bulk gas motions or turbulence on smaller scales that is causing the change in maser intensity.

Subject headings: ISM: clouds — ISM: magnetic fields — masers — polarization — radio lines: ISM — stars: formation

1. INTRODUCTION

The ability to carry out high angular resolution observations of several types of masers has increased tremendously due to the availability of interferometers at several different frequencies. For example, 36 GHz methanol maser observations are now routine with the Karl G. Jansky Very Large Array (VLA), e.g., Sjouwerman, Pihlström & Fish (2010) and Fish et al. (2011). Since masers allow for the observation of magnetic fields at high angular resolution via the Zeeman effect, there has often been speculation on whether they trace the large-scale magnetic field or only the field within the small-scale environments in which such masers form (Fish & Reid 2006; Vlemmings et al. 2010; Sarma & Momjian 2009, 2011). Since the observation of magnetic fields is challenging in general (e.g., Troland et al. 2008), the ability to measure the large-scale magnetic field with masers would prove to be invaluable,

¹National Radio Astronomy Observatory, Socorro NM 87801; emomjian@nrao.edu

²Physics Department, DePaul University, 2219 N. Kenmore Ave., Byrne Hall 211, Chicago IL 60614; asarma@depaul.edu

especially because magnetic fields play such an important role in the process of star formation (e.g., McKee & Ostriker 2007; Banerjee & Pudritz 2007).

At a distance of 450 pc (Genzel & Stutzki 1989), the Orion Molecular Cloud 2 (OMC-2) is considered one of the nearest intermediate-mass star forming regions (e.g., Takahashi et al. 2008). This region is located at an angular distance of 12' northeast of the Trapezium OB cluster, and along with OMC-3, it is part of a single long filament in Orion (Castets & Langer 1995; Chini et al. 1997). In 2011, we reported the discovery of the Zeeman effect in the 44 GHz Class I CH₃OH maser line toward OMC-2 (Sarma & Momjian 2011). In this paper, we report follow-up observations on the Zeeman effect of this methanol maser line. These observations provide the opportunity to study whether the intensity or the magnetic field has changed since our first observations (Sarma & Momjian 2011), and the implications this would have for measuring magnetic fields with 44 GHz CH₃OH masers. The observations and data reduction are presented in §2. In §3, we present the analysis to derive the line of sight magnetic field value through the Zeeman effect. Finally, we present the results and the discussion in § 4.

2. OBSERVATIONS, DATA REDUCTION

We observed the $7_0 - 6_1 A^+$ CH₃OH (methanol) maser emission line at 44 GHz with the VLA^a on 2011 September 25. The observations were carried out in dual polarization with a 1 MHz bandwidth and 256 spectral channels. At the time of the observations, the array was in the later stages of the reconfiguration from the most extended, A-configuration (maximum baseline = 36 km), to the most compact, D-configuration (maximum baseline = 1 km). On the day of the observations, all antennas except for one were already placed in D-configuration. The sole unmoved antenna that resulted in baselines \gg 1 km was edited out during the data reduction process. The total observing time was 4 hours. The calibrator source J0542+4951 (3C147) was used to derive the antenna-based amplitude gain factors to calibrate the flux density scale. The uncertainty in the flux density calibration at the observed frequency, accounting for various observational parameters (e.g., weather, reference pointing, elevation effects), is expected to be up to 10%. Table 1 summarizes the parameters of these observations.

Data reduction, including calibration, deconvolution and imaging, was carried out using the Astronomical Image Processing System (Greisen 2003). The flux density scale of the

^aThe National Radio Astronomy Observatory (NRAO) is a facility of the National Science Foundation operated under cooperative agreement by Associated Universities, Inc.

target source was set by applying the amplitude gain calibration solutions of 3C147. After Doppler correcting the data of OMC-2, the spectral channel with the brightest maser emission signal was split off, and self-calibrated in both phase and amplitude and imaged in a succession of iterative cycles. The final self-calibration solutions were applied to the full spectral-line data set of the target source. Hanning-smoothed Stokes $I=(\text{RCP}+\text{LCP})/2$ and $V=(\text{RCP}-\text{LCP})/2^{\text{b}}$ image cubes were then constructed with a synthesized beamwidth of $2.17'' \times 1.96''$, and an effective velocity resolution of 0.053 km s^{-1} . The resulting image cubes were further processed using the MIRIAD data reduction package to derive the magnetic field value.

We note that these observations are one of the first successful Zeeman effect observations and detection with the Wide-band Digital Architecture (WIDAR) correlator. In 2010, the VLA/WIDAR commissioning team discovered a small but significant unanticipated spectral response, or “spectral splatter” effect while observing strong spectral lines at high frequency resolutions. Zeeman effect studies, which in this case rely on the difference of two strong signals, were particularly vulnerable. The “spectral splatter” problem resulted in corrupt Stokes V spectra, and sometimes in false Zeeman effect detections, e.g., in the strongest 36 GHz methanol maser line in the star forming region DR21W (Fish et al. 2011; Momjian, Sjouwerman & Fish 2012). This rendered the S-curve profiles in the Stokes V data very unreliable (Sault 2010, 2012a,b). While the various Zeeman effect commissioning tests were concluded in April 2012, these tests showed that spectral line data acquired since August 2011 with WIDAR would be suitable for Zeeman effect and other spectral-line polarization studies. The OMC-2 observations reported in this paper were carried out in light of the various changes that have been implemented in the VLA/WIDAR system to address the spectral splatter problem. The data have been checked carefully to verify that the detected signal in Stokes V is astronomical in nature and not instrumental.

3. ANALYSIS

Following the arguments presented in §3 of Sarma & Momjian (2011) for maser lines with widths $\Delta\nu$ much greater than the Zeeman splitting $\Delta\nu_z$, we measured the Zeeman effect by fitting the Stokes V spectra in the least-squares sense to the equation

$$V = aI + \frac{b}{2} \frac{dI}{d\nu} \quad (1)$$

^bRCP is right- and LCP is left-circular polarization incident on the antennas. RCP has the standard radio definition of clockwise rotation of the electric vector when viewed along the direction of wave propagation.

(Troland & Heiles 1982; Sault et al. 1990), where a and b are the fit parameters. Here, a is usually the result of small calibration errors in RCP versus LCP, and it is on the order of 10^{-4} or less in our observations. The magnetic field value is obtained through the fit parameter b , where $b = zB \cos \theta$. Here, z is the Zeeman splitting factor (Hz mG^{-1}), B is the magnetic field, and θ is the angle of the magnetic field to the line of sight (Crutcher et al. 1993). The value of the Zeeman splitting factor z for CH_3OH masers is not known but is likely to be very small because CH_3OH , like H_2O , is a non-paramagnetic molecule. Therefore, we will report only values of zB_{los} . We note that while eq. (1) is true only for thermal lines, numerical solutions of radiative transfer equations (e.g., Nedoluha & Watson 1992) have shown that it also results in reasonable values for the magnetic fields in masers.

4. RESULTS AND DISCUSSION

Figure 1 (left panel) shows the Stokes I and V spectra of the 44 GHz CH_3OH maser toward OMC-2 from our current observations. As described in § 3, we determined magnetic fields by fitting the Stokes V spectra in the least-squares sense using equation (1). The fit parameter $b = zB_{\text{los}}$ (see eq. 1) obtained by this procedure is 17.7 ± 0.9 Hz. By convention, a positive value for B_{los} indicates a field pointing away from the observer.

Also shown in Figure 1 (right panel) is the Stokes I and V spectra of the same 44 GHz CH_3OH maser from Sarma & Momjian (2011). We conclude that this is the same maser as in the follow-up observations because the masers in both epochs have the same velocity (v_{LSR}), and are at the same position relative to other, weaker masers in the field. Sarma & Momjian (2011) found for this maser that $b = zB_{\text{los}} = 18.4 \pm 1.1$ Hz. Compared to Sarma & Momjian (2011), the intensity of the maser is a factor of 1.5 higher in the current observations, while the values of zB_{los} are the same, within the errors.

In order to obtain the value of B_{los} from b , we need to know the Zeeman splitting factor z . An empirical value for the Landé g -factor can be obtained by extrapolation from lab measurements of several methanol maser transitions near 25 GHz made by Jen (1951). Using this g -factor would result in a value of z for the 44 GHz methanol maser line of 0.1 Hz mG^{-1} , implying a line-of-sight magnetic field value of order 0.2 G. Such a value is an order of magnitude higher than those measured by water masers in star forming regions (e.g., Sarma et al. 2002, 2008). Moreover, the empirical scaling relation between the hydrogen molecule number density and magnetic field, $B \propto n^{0.47}$ (Crutcher 1999), would result in a number density of 10^{11} cm^{-3} , a value that is several orders of magnitude higher than that thought to be suitable for the 44 GHz methanol maser line (e.g., Pratap et al. 2008). Vlemmings et al. (2011) presented a detailed discussion on the uncertainty of the g -factor derived by Jen (1951) while

reporting the magnetic field values of various 6.7 GHz methanol masers. These authors concluded that the g -factor may be uncertain by an order of magnitude. Due to this, we have chosen to leave our results in terms of b rather than B_{los} . Our observations and the above noted considerations motivate the immediate need for an experimental measurement of the Landé g -factor in the 44 GHz methanol maser line.

With the detection of consistent Stokes V signals in the 44 GHz methanol maser line in OMC-2 through two observing epochs, it is timely to assess whether the detected signal can be attributed to a magnetic field, and therefore being due to a real Zeeman effect. As described by Vlemmings et al. (2011), a potential effect that could mimic a regular Zeeman effect is caused by a rotation of the axis of symmetry for the molecular quantum states, and can occur when the stimulated emission rate of the maser R becomes greater than the Zeeman splitting $g\Omega$ as the brightness of the maser increases while it becomes more saturated. The detected splitting in our two epoch observations (this work and Sarma & Momjian 2011) is $g\Omega \simeq 18 \text{ s}^{-1}$. The value of R can be estimated using $R \simeq AkT_{\text{b}}\Delta\Omega/4\pi h\nu$ (e.g., Vlemmings et al. 2011), where A is the Einstein coefficient for the 44 GHz methanol maser transition, which is $0.392 \times 10^{-6} \text{ s}^{-1}$ (Cragg et al. 1993), k and h are the Boltzmann and Planck constants, respectively, ν is the frequency of the maser transition, T_{b} is the maser brightness temperature, and $\Delta\Omega$ is the maser beaming solid angle. Higher angular resolution observations of the brightest 44 GHz methanol maser in OMC-2 resulted in $T_{\text{b}} = 1.74 \times 10^7 \text{ K}$ and $\Delta\Omega = 4.8 \times 10^{-3}$ (Slysh & Kalenskii 2009). From these parameters, we derive $R \sim 10^{-3} \text{ s}^{-1}$. This is several orders of magnitude lower than $g\Omega$, and suggests that the detected Stokes V signal is unlikely to be due to this non-Zeeman effect. Furthermore, this particular effect would introduce maser-intensity-dependent circular polarization because the molecules interact more strongly with the radiation field than with the magnetic field (Vlemmings et al. 2011). Since we observe no change in splitting over two epochs (Sarma & Momjian 2011 and this work) in spite of the maser intensity having increased by a factor of 1.5, this is additional proof that the detected signal is due to the Zeeman effect in a magnetic field.

As noted above, the intensity of the maser is a factor of 1.5 higher in the current observations compared to Sarma & Momjian (2011). Very few observations exist of the variability of 44 GHz Class I methanol masers, or indeed of any kind of Class I methanol maser. Such masers are believed to be excited in outflows in star forming regions. Kurtz et al. (2004) observed some variability in a number of sources, but due to differences in spatial and spectral resolution and coverage, were able to confirm variability in only two 44 GHz methanol maser sources. More recently, Pratap et al. (2007) have reported short term variability on the scales of days or possibly even hours, in 44 GHz Class I masers toward the DR21 region.

Even though the 44 GHz methanol maser intensity in OMC-2 has increased, the mea-

sured magnetic field (as given by zB_{los}) has stayed the same, within the errors. This leads us to speculate that the mechanism responsible for the change in maser intensity may be active on smaller scales than the shock compression that sets up the magnetic field. To elaborate, the post-shock magnetic field that we are detecting via the Zeeman effect was likely amplified above its pre-shock value in proportion to the density of the post- and pre-shock regions (e.g., equation (2) of Sarma & Momjian 2011). This does not appear to have changed between the two epochs, as $b = zB_{\text{los}}$ has remained the same. Meanwhile, variability in collisionally pumped masers such as the 44 GHz Class I methanol maser likely results from bulk gas flows and turbulence moving parts of the maser column in and out of velocity coherence along the line of sight (Gray 2005). Evidently, a larger column of gas has been moved into the line of sight to increase the maser intensity, but the compression factor between post- and pre-shock regions has remained the same, thereby keeping the magnetic field the same. It would be very interesting, therefore, to observe other regions and compare maser intensities and magnetic fields between epochs in order to determine how frequently this happens. If the effect were widespread, it might mean that we are detecting the large-scale magnetic field in the shocked region that is not affected by any changes on smaller scales that cause the intensity of the maser to change.

5. CONCLUSIONS

We have presented a second epoch of observations of the 44 GHz Class I methanol maser line toward the star forming region OMC-2 with the VLA. We detected a magnetic field value of $zB_{\text{los}} = 17.7 \pm 0.9$ Hz. The observations constitute one of the first successful Zeeman effect detections with the new WIDAR correlator of the VLA. Comparing to the result of our earlier epoch of data for this region (Sarma & Momjian 2011), we find that the intensity of the maser has changed by a factor of 1.5, but the magnetic field value has stayed the same, within the errors. We speculate that we may be detecting the large-scale magnetic field in the post-shock region that is unaffected by bulk motions or turbulence on smaller scales that may be causing the change in the maser intensity.

REFERENCES

- Banerjee, R., & Pudritz, R. E. 2007, *ApJ*, 660, 479
- Castets, A., & Langer, W. D. 1995, *A&A*, 294, 835
- Chini, R., et al. 1997, *ApJ*, 474, L135
- Cragg, D. M., Mikhtiev, M. A., Bettens, R. P. A., Godfrey, P. D., & Brown, R. D. 1993, *MNRAS*, 264, 769
- Crutcher, R. M., Troland, T. H., Goodman, A. A., Heiles, C., Kazes, I., & Myers, P. C. 1993, *ApJ*, 407, 175
- Crutcher, R. M. 1999, *ApJ*, 520, 706
- Fish, V. L., & Reid, M. J. 2006, *ApJS*, 164, 99
- Fish, V. L., Muehlbrad, T.C., Pratap, P., Sjouwerman, L.O., Strel'nitski, V., Pihlström, Y.M., & Bourke, T.L., 2011, *ApJ*, 729, 14
- Genzel, R., & Stutzki, J. 1989, *ARA&A*, 27, 41
- Gray, M. 2005, *Ap&SS*, 295, 309
- Greisen, E. W. 2003, *Information Handling in Astronomy - Historical Vistas*, 285, 109
- Jen, C. K. 1951, *Physical Review*, 81, 197
- Kurtz, S., Hofner, P., & Álvarez, C. V. 2004, *ApJS*, 155, 149
- Momjian, E., Sjouwerman, L. O., & Fish, V. L. 2012, *ApJ*, in press.
- McKee, C. F., & Ostriker, E. C. 2007, *ARA&A*, 45, 565
- Nedoluha, G. E., & Watson, W. D. 1992, *ApJ*, 384, 185
- Pratap, P., Strel'nitski, V., Hoffman, S., & Lemonias, J. 2007, *IAU Symposium*, 242, 34
- Pratap, P., Shute, P. A., Keane, T. C., Battersby, C., & Sterling, S. 2008, *AJ*, 135, 1718
- Sarma, A. P., Troland, T. H., Crutcher, R. M., & Roberts, D. A. 2002, *ApJ*, 580, 928
- Sarma, A. P., Troland, T. H., Romney, J. D., & Huynh, T. H. 2008, *ApJ*, 674, 295
- Sarma, A. P., & Momjian, E. 2009, *ApJ*, 705, L176

- Sarma, A. P., & Momjian, E. 2011, *ApJ*, 730, L5
- Sault, R. J., Killeen, N. E. B., Zmuidzinas, J., & Loushin, R. 1990, *ApJS*, 74, 437
- Sault, R.J. 2010, EVLA Memo 148 (<http://www.aoc.nrao.edu/evla/memolist.shtml>)
- Sault, R.J. 2012a, EVLA Memo 157 (<http://www.aoc.nrao.edu/evla/memolist.shtml>)
- Sault, R.J. 2012b, EVLA Memo 160 (<http://www.aoc.nrao.edu/evla/memolist.shtml>)
- Sjouwerman, L.O., Pihlström, Y.M., & Fish, V.L. 2010, *ApJ*, 710, L111
- Slysh, V. I., & Kalenskii, S. V. 2009, *Astronomy Reports*, 53, 519
- Takahashi, S., Saito, M., Ohashi, N., Kusakabe, N., Takakuwa, S., Shimajiri, Y., Tamura, M., & Kawabe, R. 2008, *ApJ*, 688, 344
- Troland, T. H., & Heiles, C. 1982, *ApJ*, 252, 179
- Troland, T. H., Heiles, C., Sarma, A. P., Ferland, G. J., Crutcher, R. M., & Brogan, C. L. 2008, arXiv:0804.3396
- Vlemmings, W. H. T., Surcis, G., Torstensson, K. J. E., & van Langevelde, H. J. 2010, *MNRAS*, 404, 134
- Vlemmings, W. H. T., Torres, R. M., & Dodson, R. 2011, *A&A*, 529, A95

Table 1. Parameters for VLA Observations

Parameter	Value
Observation Date	2011 Sep 25
Configuration	D
R.A. of field center (J2000)	05 ^h 35 ^m 27 ^s .66
Decl. of field center (J2000)	−05°09′39″.6
Total Bandwidth	1 MHz
No. of channels	256
Total Observing Time	4 hr
Rest Frequency	44.069488 GHz
Target source velocity	11.6 km s ^{−1}
Hanning Smoothing	Yes
Effective velocity resolution	0.053 km s ^{−1}
FWHM of synthesized beam	2.17″ × 1.96″
	P.A. = 15°
Line rms noise ^a	10 mJy beam ^{−1}

^aThe line rms noise was measured from the stokes *I* image cube using maser line free channels.

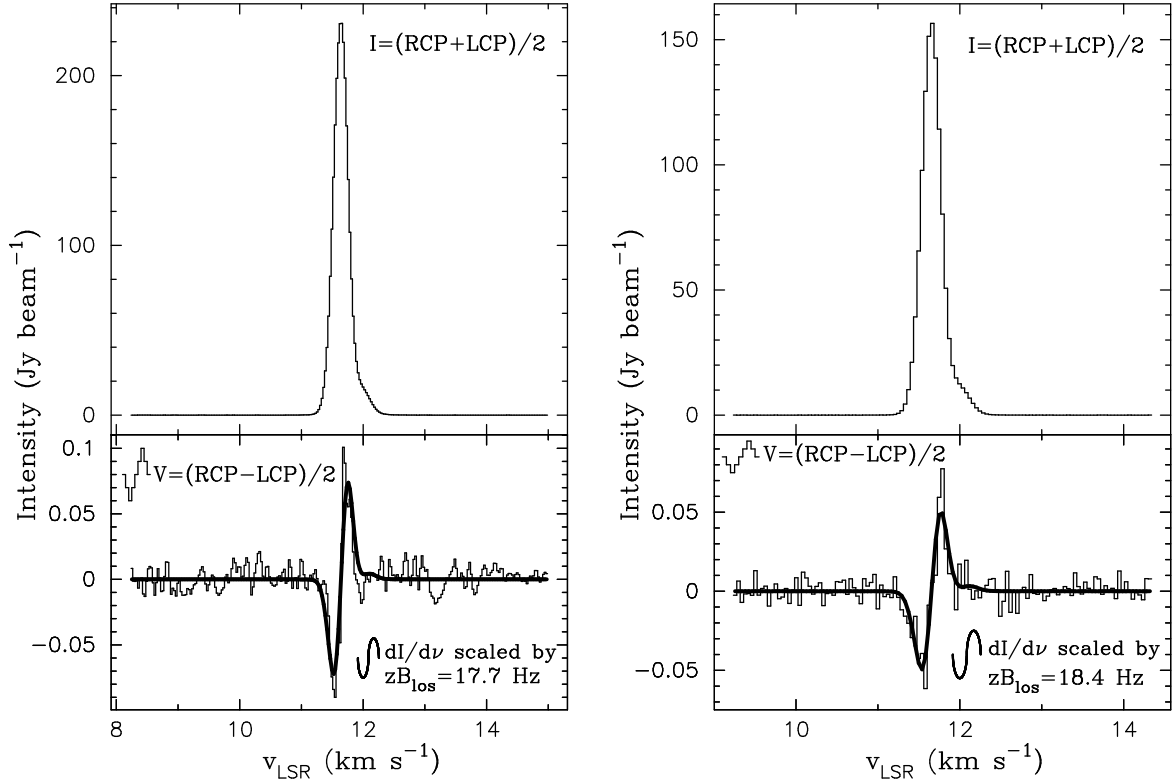


Fig. 1.— Stokes I (*top-histogram*) and V (*bottom-histogram*) profiles of the maser toward the 44 GHz Class I CH_3OH maser in OMC-2. The left panel shows the data from our current observations, and the right displays the data from Sarma & Momjian (2011). The curve superposed on V in the lower frame is the derivative of I scaled by a value of $zB_{\text{los}} = 17.7 \pm 0.9$ Hz in the left panel and $zB_{\text{los}} = 18.4 \pm 1.1$ Hz in the right panel respectively.